Brain, Behavior, and Immunity 111 (2023) 32–45

Contents lists available at ScienceDirect

Brain Behavior and Immunity

journal homepage: www.elsevier.com/locate/ybrbi

Analyzing schizophrenia-related phenotypes in mice caused by autoantibodies against NRXN1α in schizophrenia

Hiroki Shiwaku [a,*], Shingo Katayama [a], Mengxuan Gao [b], Kanoh Kondo [c], Yuri Nakano [a], Yukiko Motokawa [a], Saori Toyoda [a], Fuyuko Yoshida [d], Hiroaki Hori [d], Tetsuo Kubota [e], Kinya Ishikawa [f], Hiroshi Kunugi [g], Yuji Ikegaya [b,h,i], Hitoshi Okazawa [c], Hidehiko Takahashi [a]

[a] Department of Psychiatry and Behavioral Sciences, Tokyo Medical and Dental University Graduate School, Tokyo 113-8510, Japan
[b] Graduate School of Pharmaceutical Sciences, The University of Tokyo, Tokyo 113-0033, Japan
[c] Department of Neuropathology, Medical Research Institute and Center for Brain Integration Research, Tokyo Medical and Dental University, 1-5-45, Tokyo 113-8510, Japan
[d] Department of Behavioral Medicine, National Institute of Mental Health, National Center of Neurology and Psychiatry, 4-1-1, Tokyo 187-8553, Japan
[e] Department of Medical Technology, Tsukuba International University, Ibaraki 300-0051, Japan
[f] The Center for Personalized Medicine for Healthy Aging, Tokyo Medical and Dental University, Tokyo 113-8510, Japan
[g] Department of Psychiatry, Teikyo University School of Medicine, Tokyo 173-8605, Japan
[h] Institute for AI and Beyond, The University of Tokyo, Tokyo 113-0033, Japan
[i] Center for Information and Neural Networks, National Institute of Information and Communications Technology, Suita City, Osaka 565-0871, Japan

ARTICLE INFO

Keywords:
Schizophrenia
Neurexin
NRXN1
anti-NRXN1α autoantibody
Autoimmune psychosis

ABSTRACT

The molecular pathological mechanisms underlying schizophrenia remain unclear; however, genomic analysis has identified genes encoding important risk molecules. One such molecule is neurexin 1α (NRXN1α), a presynaptic cell adhesion molecule. In addition, novel autoantibodies that target the nervous system have been found in patients with encephalitis and neurological disorders. Some of these autoantibodies inhibit synaptic antigen molecules. Studies have examined the association between schizophrenia and autoimmunity; however, the pathological data remain unclear. Here, we identified a novel autoantibody against NRXN1α in patients with schizophrenia (n = 2.1%) in a Japanese cohort (n = 387). None of the healthy control participants (n = 362) were positive for anti-NRXN1α autoantibodies. Anti-NRXN1α autoantibodies isolated from patients with schizophrenia inhibited the molecular interaction between NRXN1α and Neuroligin 1 (NLGN1) and between NRXN1α and Neuroligin 2 (NLGN2). Additionally, these autoantibodies reduced the frequency of the miniature excitatory postsynaptic current in the frontal cortex of mice. Administration of anti-NRXN1α autoantibodies from patients with schizophrenia into the cerebrospinal fluid of mice reduced the number of spines/synapses in the frontal cortex and induced schizophrenia-related behaviors such as reduced cognition, impaired pre-pulse inhibition, and reduced social novelty preference. These changes were improved through the removal of anti-NRXN1α autoantibodies from the IgG fraction of patients with schizophrenia. These findings demonstrate that anti-NRXN1α autoantibodies transferred from patients with schizophrenia cause schizophrenia-related pathology in mice. Removal of anti-NRXN1α autoantibodies may be a therapeutic target for a subgroup of patients who are positive for these autoantibodies.

1. Introduction

The pathological mechanisms underlying schizophrenia remain unclear. This disease entity is believed to comprise heterogeneous pathologies and multiple subgroups (Meyer-Lindenberg, 2010). Genetic studies have identified several susceptible loci and genes associated with schizophrenia (Consortium, 2014; Marshall et al., 2017; Tromp et al., 2021). For example, among the eight disease-susceptible loci identified from a large cohort study, 2p16.3 was highlighted because only the *neurexin 1* (*NRXN1*) gene resides in the region, and its odds ratio (OR:

Abbreviations: NRXN1, neurexin 1.

* Corresponding author.
E-mail address: shiwaku.npat@mri.tmd.ac.jp (H. Shiwaku).

https://doi.org/10.1016/j.bbi.2023.03.028
Received 5 August 2022; Received in revised form 24 March 2023; Accepted 28 March 2023
Available online 31 March 2023

14.4) for schizophrenia was one of the highest (Marshall et al., 2017). Similar ORs were reported by other studies, suggesting that neurexin 1α (NRXN1α) is a key molecule that can influence the molecular pathology of schizophrenia (Hu et al., 2019; Singh et al., 2022; Tromp et al., 2021; Vrijenhoek et al., 2008; Walsh et al., 2008). In addition to schizophrenia, NRXN1α mutations can also be a risk factor for autism spectrum disorder and intellectual disability (Lowther et al., 2017; Szatmari et al., 2007; Zahir et al., 2008).

NRXN1α is a pre-synapse adhesion molecule that interacts with post-synapse adhesion molecules such as neuroligins (NLGNs) (Dean and Dresbach, 2006; Südhof, 2017). NRXN1α acts as a platform and hub for synaptic molecular interactions and signaling (Dean and Dresbach, 2006; Südhof, 2017). Thus, it is reasonable to assume that NRXN1α dysfunction plays a role in the development of psychiatric disorders such as schizophrenia.

Autoantibodies or autoimmunity are suspected pathologies of schizophrenia (Consortium, 2014; Cullen et al., 2019). Autoantibodies against membrane molecules of the nervous system have been discovered in patients with encephalitis (Dalmau, 2016; Prüss, 2021). Thus, we searched for novel autoantibodies against synaptic molecules under the assumption that autoantibodies against synaptic membrane molecules in patients with schizophrenia could be involved in the pathogenesis of schizophrenia (Shiwaku et al., 2022). As a result, we found novel autoantibodies against Neural cell adhesion molecule 1 (NCAM1) in patients with schizophrenia and showed that anti-NCAM1 autoantibodies induce schizophrenia-related synaptic and behavioral pathologies in mice. Namely, as with anti-*N*-methyl-D-aspartate (NMDA) receptor autoantibodies, anti-NCAM1 autoantibodies also inhibit NCAM1 function, resulting in pathology (Shiwaku et al., 2022). In this screening, one of the targets of analysis was NRXN1α, and this study focuses on the detailed analysis of this autoantibody.

Here, we identified novel autoantibodies against NRXN1α in some patients with schizophrenia. Autoantibodies against NRXN1α have not been reported thus far, even in patients with encephalitis. Using a disease model in which mice were administered IgG purified from the serum of patients with schizophrenia, we showed that anti-NRXN1α autoantibodies interrupt the molecular interactions of NRXN1α, alter electrophysiological and synaptic properties, reduce the number of spines/synapses in the frontal cortex, and cause schizophrenia-related behaviors.

2. Methods

2.1. Participants

Serum was obtained from 387 patients with schizophrenia and 362 healthy controls. The participants were inpatients from Tokyo Medical and Dental University Medical Hospital, Kurita Hospital, and Takatsuki Hospital, and patients from the outpatient clinic of the National Center of Neurology and Psychiatry Hospital between April 1, 2016, and December 31, 2021. All were diagnosed with schizophrenia according to the Diagnostic and Statistical Manual of Mental Disorders (DSM-5) criteria. None of the healthy controls had a previous history of psychiatric disorders. Healthy control sera were obtained from healthy volunteers and BioBank at the Bioresource Research Center, Tokyo Medical and Dental University. All participants were Japanese.

2.2. Ethics

This study was performed in strict accordance with the Guidelines for Proper Conduct of Animal Experiments by the Science Council of Japan, the Helsinki Declaration, and the Ethical Guidelines for Medical and Health Research Involving Human Subjects in Japan. It was approved by the Committees on Gene Recombination Experiments, Human Ethics, and Animal Experiments of the Tokyo Medical and Dental University (G2020-002A, M2000-1866, and A2020-113A). All participants provided written informed consent.

2.3. Serum samples and CSF samples

Serum samples were collected in the morning following an overnight fast or more than 2 h after eating. CSF samples were also collected from patients with schizophrenia with anti-NRXN1α autoantibodies in the morning within a month after serum samples were collected. The serum and CSF were aliquoted and stored in a − 80 °C freezer. Cell-based assays and enzyme-linked immunosorbent assay (ELISA) were performed with newly thawed samples, avoiding freeze and thaw. As for CSF testing, total protein, albumin, glucose, IgG, and leukocyte numbers in CSF were analyzed by the clinical laboratory testing company (SRL, Tokyo, Japan).

2.4. Cell culture and transfection

HeLa cells were maintained at 37 °C/5% CO_2 in Dulbecco's Modified Eagle Medium (SIGMA, MI, USA) supplemented with 10% fetal bovine serum (FBS). Cells were transfected with plasmids using Lipofectamine 2000 (Thermo Fisher Scientific, Waltham, MA, USA), according to the manufacturer's protocol. Mouse primary cerebral neurons were prepared from embryonic-day 15 C57BL/6J mouse embryos. Cerebral cortexes (n = 4–6) were dissected, incubated with 0.05% trypsin in 4 mL of phosphate-buffered saline (PBS) (Thermo Fisher Scientific, Waltham, MA, USA) at 37 °C for 15 min, and dissociated by pipetting. The cells were passed through a 70-μm cell strainer (Thermo Fisher Scientific, Waltham, MA, USA), collected by centrifugation, and cultured in neurobasal medium (Thermo Fisher Scientific, Waltham, MA, USA) containing 2% B27, 0.5 mM L-glutamine, and 1% penicillin/streptomycin in the presence of 0.5 μM AraC. Immunohistochemistry of primary neurons was performed at 14 days (DIV 14).

2.5. Construction of DNA vectors

NRXN1α and enhanced green fluorescent protein (EGFP) were cloned into a pRP vector (VectorBuilder, TX, USA), and expression was driven by the cytomegalovirus (CMV) promoter (Supplementary Fig. 1A). NRXN1α deletion constructs were generated using PrimeSTAR Max DNA Polymerase (Takara, Tokyo, Japan) and primers (Supplementary Table 2).

2.6. ELISA analysis

Polystyrene microtiter plates (3455, Thermo Scientific, Waltham, MA, USA) were coated with 100 μL (2 μg/mL) of NRXN1α recombinant protein (TP319376, Origene) in Tris-Buffered Saline (TBS) buffer and incubated overnight at 4 °C. The plates were washed three times with TBS and then incubated for 1 h at 24 °C with 100 μL/well TBS containing 1% BSA to block nonspecific binding. These were then incubated for 1 h at 24 °C with 100 μL of each dilution of serum and CSF samples (1:50 for serum and 1:1 for CSF in TBS containing 1% BSA). The plates were washed three times with TBS containing 0.1% Tween 20 and then incubated with anti-human IgG-alkaline phosphatase (1:50000; Cat# 2064, Sigma-Aldrich) in TBS containing 0.1% Tween 20 for 1 h at room temperature. After washing with TBS, 1 mg/mL p-nitrophenyl phosphate in substrate buffer (N1891, Sigma-Aldrich) was added to each well. Absorbance at 405 nm was read on a microplate reader (Spark 10 M, TECAN).

2.7. Western blot analysis

Samples were lysed in 62.5 mM Tris-HCl, pH 6.8, 2% (w/v) sodium dodecyl sulfate (SDS), 2.5% (v/v) 2-mercaptoethanol, 5% (v/v) glycerin, and 0.0025% (w/v) bromophenol blue. Samples were separated by sodium dodecyl sulfate polyacrylamide gel electrophoresis (SDS–PAGE),

transferred onto Immobilon-P Transfer Membranes (Merck Millipore, Burlington, MA, USA) using a semi-dry method, and blocked with 5% milk in TBS/Tween 20 (TBST) (10 mM Tris/Cl, pH 8.0, 150 mM NaCl, and 0.05% Tween 20). The filters were incubated overnight at 4 °C with each primary antibody. The following primary antibodies were diluted in Can Get Signal solution (Toyobo, Osaka, Japan): anti-NRXN1α (1:1000; ANR-031, Alomone Labs); anti-Myc (1:2000; M047-3, MBL, Tokyo, Japan); anti-NLGN1 (1:1000; ANR-035, Alomone Labs); anti-NLGN2 (1:1000; 129203, Synaptic Systems); anti-His (1:1000; 46–0693, Thermo Scientific, Waltham, MA, USA); and anti-β-actin (1:3000; sc-47778, Santa Cruz Biotechnology). Secondary antibodies were HRP-linked anti-rabbit IgG (1:3000; NA934, GE Healthcare, Chicago, IL, USA) and HRP-linked anti-mouse IgG (1:3000; NA931, GE Healthcare, Chicago, IL, USA). Proteins were detected using ECL Prime Western Blotting Detection Reagent (RPN2232, GE Healthcare, Chicago, IL, USA) and a luminescence image analyzer (ImageQuant LAS 500, GE Healthcare, Chicago, IL, USA).

2.8. Immunocytochemistry, immunohistochemistry, and cell-based assays

HeLa cells and primary cortical neurons were fixed for 30 min at room temperature in 2% paraformaldehyde (prepared in phosphate buffer), treated for 10 min with 0.1% Triton X-100 in PBS, blocked for 30 min at room temperature with PBS containing 10% FBS or 1% BSA, and then incubated with either serum or primary antibody diluted in blocking buffer. For the live cell-based assay, HeLa cells or primary cortical neurons were incubated without fixation for 1 h and then fixed for 30 min at room temperature in 2% paraformaldehyde. Serum with an autoantibody titer $\geq$ 1:30 was defined as autoantibody-positive. Previous studies show that NMDA receptor autoantibody, gamma-aminobutyric acid (GABA) receptor autoantibody, and NCAM1 autoantibody titers are usually higher than 1:30 (Pettingill et al., 2015; Shiwaku et al., 2022; Shiwaku et al., 2020; Steiner et al., 2013). Furthermore, diluting the serum has the advantage of preventing nonspecific staining.

For immunohistochemistry, brain samples were fixed with 4% paraformaldehyde and embedded in paraffin. Sagittal or coronal sections (5-μm thick) were cut using a microtome (Microm HM 335 E, GMI, Ramsey, USA). Immunohistochemistry was performed using the following primary antibodies: anti-NRXN1α (1:250; ANR-031, Alomone labs); anti-NRXN1 (1:250, CSB-PA347832LA01HU, CUSABIO); anti-PSD95 (1:200, D74D3, Cell signaling); anti-gephyrin (1:200, 147011, Synaptic Systems); anti-vGLUT1 (1:200, 135011, Synaptic Systems); anti-SV2 (1:200, E-8, sc-376234, Santa Cruz Biotechnology), anti-NFκB p65 (1:200, sc-372, Santa Cruz Biotechnology); and anti-Iba1 (1:200, 019-19741, WAKO). These were detected using Cy3-conjugated anti-human IgG (1:500, 709-165-149, Jackson Laboratory, Bar Harbor, ME, USA); Alexa Fluor 488-conjugated anti-rabbit IgG (1:500, A21206, Thermo Scientific, Waltham, MA, USA); and a Zenon Alexa Fluor 568 Rabbit IgG Labeling Kit (Thermo Fisher Scientific, Z2505306, Waltham, MA, USA). Nuclei were stained with 4′,6-diamidino-2-phenylindole (0.2 μg/mL in PBS; DOJINDO). Images were acquired under an Olympus FV1200 confocal microscope (Tokyo, Japan). Blinded observers performed image acquisition and manually counted the synaptic puncta of PSD95, VGLUT1, gephyrin, and SV2A.

2.9. Electrophysiological analysis

Acute slices were prepared from post-natal week 3–4 ICR mice of both sexes (SLC, Shizuoka, Japan). Mice were anesthetized with isoflurane and then decapitated. The brain was placed in an ice-cold, oxygenated cutting solution containing the following: 27 mM $NaHCO_3$, 1.5 mM NaH_2PO_4, 2.5 mM KCl, 0.5 mM ascorbic acid, 1 mM $CaCl_2$, 7 mM $MgSO_4$, and 222.1 mM sucrose. The brain was sliced coronally at a thickness of 400 μm and a speed of 0.08 mm/s using a vibratome (VT1200S; Leica Microsystems, Nussloch, Germany). The slices were allowed to recover at 35 °C for 15–20 min and then at room temperature in oxygenated artificial cerebrospinal fluid (aCSF) containing the following: 127 mM NaCl, 26 mM $NaHCO_3$, 3.5 mM KCl, 1.24 mM NaH_2PO_4, 1.3 mM $MgSO_4$, 2.4 mM $CaCl_2$, and 10 mM glucose; serum obtained from a healthy participant or patients with schizophrenia was added to the aCSF (final dilution, 1:1000). Recordings were performed in a submerged chamber perfused (3–5 mL/min) with oxygenated aCSF at room temperature. During the application of 1 μM tetrodotoxin (TTX; Tocris Bioscience), whole-cell patch-clamp recordings were obtained from layer 2/3 ACC pyramidal cells, which were identified visually under an infrared differential interference contrast microscope. Borosilicate glass pipettes (4–7 MΩ) were filled with a Cs-based solution containing the following: 130 mM $CsMeSO_4$, 10 mM CsCl, 10 mM HEPES, 10 mM phosphocreatine, 4 mM MgATP, 0.3 mM NaGTP, and 10 mM QX-314. Cells were discarded if the mean resting potential was more positive than −50 mV. Miniature excitatory or inhibitory postsynaptic currents (mEPSCs or mIPSCs) were recorded under voltage clamp mode at −70 or 0 mV, respectively. The signals were amplified and digitized at a sampling rate of 20 kHz using a MultiClamp 700B amplifier and a Digidata 1440A digitizer, which were controlled using pCLAMP 10.3 software (Molecular Devices). The data were exported at 20 kHz and processed with custom-made routines in MATLAB R2016a (MathWorks, Natick, MA, USA). To determine the threshold of mEPSCs and mIPSCs, data points of the membrane current trace were arranged according to amplitude after humming noise reduction (45–55 Hz) using a band-pass filter; the standard deviation (SD) of the 10–50% amplitude range was then calculated. mEPSCs or mIPSCs >5 × SD were detected.

2.10. Mice

C57BL/6J mice were obtained from CLEA Japan (Tokyo, Japan). Mice were housed in standard cages in a temperature- and humidity-controlled room with a 12-h light/dark cycle (lights on at 08:00). Purified human IgGs were injected into the subarachnoid space of the frontal cortex of 8-week-old mice. Molecular, histological, two-photon microscopy, and behavioral analyses were performed in 9-week-old mice. Investigators were blinded regarding the treatment of mice when performing experiments and analyzing data.

2.11. Behavioral tests

All behavioral tests were analyzed using a video-computerized tracking system (SMART, Panlab, Barcelona, Spain). All behavioral tests were performed using male C57BL/6J mice and female C57BL/6J mice, as shown in Supplementary Fig. 8.

2.11.1. Open-field test

Mice were placed in an open-field box (40 × 40 × 22 cm) and allowed to explore freely for 10 min. The total distance traveled and the time spent in the central zone (20 × 20 cm) were measured.

2.11.2. Three-chamber sociability test

Mice were placed in a three-chambered box. Each chamber measured 40 cm × 20 cm × 22 cm (*L, W, H*). The dividing chamber walls contained openings allowing access into each chamber. The test comprised three sessions. During the first session (habituation), the mouse was allowed to explore three chambers for 5 min; then, the mouse was confined in the central chamber for another 5 min. In the following session (sociability), an unfamiliar mouse was placed in the wire cup in one of the side chambers, and the test mouse was allowed to freely explore all three chambers for 10 min. In the last (social novelty preference) session, a new, unfamiliar mouse was placed in the wire cup in the opposite-side chamber, and the test mouse was allowed to freely explore all three chambers for 10 min. The time spent in each chamber and the actual interaction time were recorded. The interaction time in the figure is based on actual interaction time.

2.11.3. Elevated plus maze test

The elevated plus maze comprised two open arms and two closed arms (30 × 6 cm; 15 cm walls; apparatus suspended 50 cm above the floor). Mice were placed in the central square of the maze, and activity was recorded for 5 min. Time spent in the open and closed arms was measured.

2.11.4. Pre-pulse inhibition test

The test was conducted using sound-attenuating startle boxes (Panlab, Barcelona, Spain). After acclimating for 5 min with background noise (65 dB), the mouse was exposed to 10 blocks of six types of startle stimuli in a pseudorandomized order. The trial types were as follows: startle-only; 40 ms, 120-dB sound burst; five pre-pulse trials; and 120-dB startle stimulus preceded 100 ms earlier by 20 ms pre-pulses (69, 73, 77, 81, or 85 dB). The maximum startle response was recorded for each startle stimulus.

2.11.5. Y-maze test

Mice were placed at the end of one arm and allowed to move freely through the maze during an 8-min session. The percentage of spontaneous alterations (indicated as an alteration rate) was calculated by dividing the number of entries into a new arm different from the previous one by the total number of transfers from one arm to another arm.

2.11.6. Novel object recognition test

During the training session, two identical objects were used, and mice were allowed to explore for 10 min. Then, one of the objects was replaced by a novel object, and mice were allowed to explore again immediately to reach the 30-s criterion of total exploration.

2.11.7. Analysis of olfactory function

Analysis was performed using cages for the three-chamber test. After the same paradigm of habituation (see the methods of the three-chamber sociability test), cotton with or without mouse scent was placed in each cup in the three-chamber test cages, and the test mouse was allowed to freely explore all three chambers for 10 min.

2.11.8. Analysis of aggressive behavior

A 7-week-old male mouse was introduced into the cage (30 × 20 × 17 cm, 20 lx) of the subject mouse. Mice were allowed to freely explore for 5 min, and the duration of the attack was manually recorded.

Mice were placed at the end of one arm and allowed to move freely through the maze during an 8-min session.

2.12. Pull-down assay

Purified IgGs (12 μg), His-NLGN1 (250 ng) (11617-H08H, SinoBiological) or His-NLGN2 (250 ng) (5645-NL, R&D Systems), and Myc-NRXN1α (250 ng) (TP319376, Origene) were mixed in 400 μL of TBS and incubated at 4 °C for 12 h. After the addition of 50-μL Ni-NTA agarose (Qiagen, Hilden, Germany), the mixtures were incubated for a further 3 h at 4 °C, centrifuged, and washed five times with TBS. For pull-down by Myc, the c-Myc-tagged protein mild purification kit (3305, MBL, Tokyo, Japan) was used. Next, the beads were mixed with an equal volume of sample buffer (62.5 mM Tris-HCl, pH 6.8, 2% (w/v) SDS, 2.5% (v/v) 2-mercaptoethanol, 5% (v/v) glycerol, and 0.0025% (w/v) bromophenol blue) and boiled at 95 °C for 10 min.

2.13. Immunoprecipitation

Mouse cerebral frontal cortex was lysed in a homogenizer with lysis buffer (20 mM Tris-HCl, pH 7.5, 100 mM NaCl, 20 mM $NahCO_3$, 4 mM KCL, 2.5 mM $MgCl_2$, 2.5 mM $CaCl_2$, 10% glycerol, 1% Triton X-100, 1% CHAPS, and 0.5% protease inhibitor cocktail [539134, Calbiochem, San Diego, CA, USA]). Lysates were rotated for 60 min at 4 °C and then centrifuged (16,000 g × 10 min at 4 °C). Lysates were incubated with 1 μg of anti-NRXN1α antibodies (NR-031, Alomone Labs, and sc-136001, Santa Cruz Biotechnology) for 16 h at 4 °C with rotation. Then, lysates were incubated with G-Sepharose beads (17061801, GE Healthcare) for 2 h, and then the beads were washed four times with lysis buffer. Bound proteins were eluted in a sample buffer (125 mM Tris-HCl, pH 6.8, 4% SDS, 10% glycerol, 0.005% BPB, and 5% 2-mercaptoethanol), separated on SDS–PAGE, and blotted with antibodies.

2.14. Purification of IgG from serum

IgG was purified from serum using Protein G HP SpinTrap columns (28903134, Cytiva, USA) according to the manufacturer's protocol.

2.15. Intrathecal injection of IgG

Mice were anesthetized with 1% isoflurane using a small animal anesthetizer (TK-7, BioMachinery, Japan). Using an injection needle made with a micropipette puller (model P-1000, Sutter Instrument, USA) and FemtoJet (Eppendorf, NY, USA), purified IgG (3 μg in 2 μL) from the serum of healthy controls or patients with schizophrenia was injected at the speed of 1 μL/min into the subarachnoid space of the frontal cortex of 8-week-old mice. Assuming a mouse CSF volume of 40 μL (Pardridge, 2016), the dilution rate used for purification and injection corresponded to a 100- to 200-fold dilution of the serum. Because the antibody titer of anti-NRXN1α autoantibodies in serum is 1:300–1:1000, we considered that the dilution rate used was appropriate for autoantibody analysis.

2.16. Two-photon microscopic analysis

This procedure has been described previously (Tanaka et al., 2018; Yang et al., 2010). Briefly, adeno-associated virus 1 (AAV1)-EGFP harboring the synapsin I promoter (titer: 1×10^{10} vector genomes/mL; 1 μL) and AAV2-VAMP2-mCherry harboring the CMV promoter were injected into adjacent positions in the frontal cortex (+1.0 mm from the bregma (mediolateral 0.5 mm; depth, 1 mm; and + 3.0 mm from the bregma [mediolateral 0.5 mm; depth, 1 mm], respectively) under anesthesia with 1% isoflurane.

Two-photon imaging was performed using a laser-scanning microscope system, FV1000MPE2 (Olympus, Tokyo, Japan), equipped with an upright microscope (BX61WI, Olympus, Japan), a water-immersion objective lens (XLPlanN25 × W; numerical aperture, 1.05) and a pulsed laser (MaiTaiHP DeepSee, Spectra-Physics, Santa Clara, CA, USA). EGFP and mCherry were excited at 920 nm and scanned at 495–540 nm and 575–630 nm, respectively. High-magnification imaging (101.28 μm × 101.28 μm; 1024 × 1024 pixels; 1-μm Z step) of cortical layer I was performed with a 5 × digital zoom through a thinned-skull window in the frontal cortex. Blinded observers performed image acquisition and analysis. The subtypes of spines (thin, mushroom, and stubby) are analyzed based on head volumes and spine length. Image processing was performed with Imaris Interactive Microscopy Image Analysis software (Bitplane, Zurich, Switzerland).

2.17. Real-time reverse transcription-quantitative polymerase chain reaction (qRT-PCR)

The total RNA was prepared from the frontal cortex of mice using an RNeasy Mini Kit (74104, QIAGEN). Reverse transcription was performed using the SuperScript VILO cDNA synthesis kit (11754–250, Invitrogen, USA). Real-time qRT-PCR was performed using a LightCycler (Roche Diagnostics, Germany) and a Thunderbird SYBR qPCR mix (Toyobo, Osaka, Japan), according to the manufacturer's protocol. The expression of individual genes was normalized to that of glyceraldehyde-3-phosphate dehydrogenase. qRT-PCR was performed using the primers listed in Supplementary Table 2.

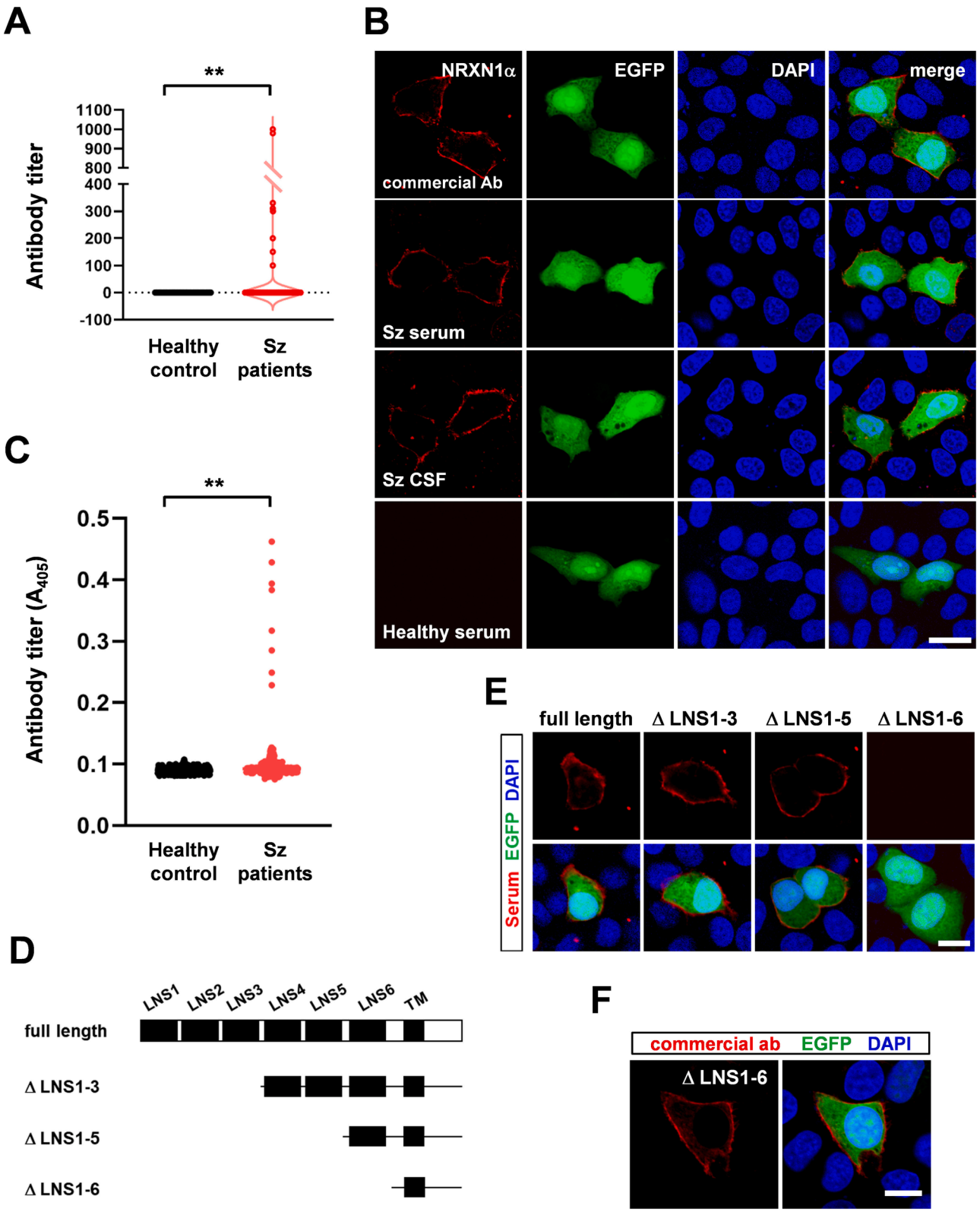

Fig. 1. Identification of anti-NRXN1α autoantibodies. A. Titers of anti-NRXN1α autoantibodies in serum by cell-based assay. $^{**}p < 0.01$ ($N = 362$ healthy controls; $N = 387$ patients with schizophrenia; Mann–Whitney U test). B. Immunocytochemistry using a commercial anti-NRXN1α antibody. Serum and CSF were used from a schizophrenia patient 1, and serum was used from healthy controls. c. Titers of anti-NRXN1α autoantibodies in serum by enzyme-linked immunosorbent assay (ELISA). $^{**}p < 0.01$ ($N = 362$; healthy controls; $N = 387$; patients with schizophrenia, Mann–Whitney U test). D. NRXN1α deletion constructs. E. Immunocytochemistry using serum from patient 1 with schizophrenia, who was positive for anti-NRXN1α autoantibodies. NRXN1α deletion constructs and EGFP were expressed from a plasmid. Similar results were obtained from all anti-NRXN1α antibody-positive patients with schizophrenia. Bar: 10 μm. F. Immunocytochemical confirmation of the expression of NRXN1αΔLNS1-6 using a commercial anti-NRXN1α antibody. Bar: 10 μm.

Table 1
Clinical characteristics of antibody-positive patients.

Case no./sex/age	Illness duration (years)	Antibody titer (CBA) (serum/CSF)	EEG	Neuroimaging	PANSS Score, Comorbidity
1/F/28	14	1000/3	Normal	MRI, no special notes	Total; 99, P, 26; N, 24; G, 49
2/F/39	11	1000/3	Normal	MRI, no special notes	Total; 85, P, 25; N, 20; G, 40
3/M/41	27	300/2	Normal	MRI, no special notes	Total; 77, P, 19; N, 15; G, 43
4/F/72	53	300/2	Normal (use of antiepileptic drugs)	MRI, no special notes	Total; 93, P, 23; N, 22; G, 48, epilepsy
5/M/37	18	300/NA	NA	MRI, no special notes	Total; 70, P, 14; N, 22; G, 34
6/F/55	30	200/1	Normal	MRI, no special notes	Total; 73, P, 20; N, 15; G, 38
7/M/23	9	100/NA	NA	MRI, no special notes	Total; 71, P, 16; N, 18; G, 37
8/M/56	31	100/1	Normal	MRI, no special notes	Total; 85, P, 22; N, 23; G, 41

EEG, electroencephalogram; F, female; M, male; MRI, magnetic resonance imaging; CSF, cerebrospinal fluid; CBA, cell based assay; NA, not available; PANSS, Positive and Negative Syndrome Scale, P, Positive symptom score; N, Negative symptom score; G, Global score.

2.18. Magnetic resonance images

The presence or absence of clinically apparent atrophy and findings suggestive of encephalitis (T2-weighted fluid-attenuated inversion recovery hyperintensity) were assessed by clinical radiologists and authors.

2.19. Statistical analysis

Statistical analysis was performed using GraphPad Prism 8.4.3 (GraphPad Software, Inc., CA, USA). ELISA and cell-based assay data were analyzed using a Mann–Whitney *U* test. Data groups were compared using Tukey's honestly significant difference (HSD) test unless otherwise noted in the figure legends. The sample size was determined based on our previous studies (Tanaka et al., 2018). All experiments were randomized. Statistical significance was set at a p-value < 0.05. The exact value of n, the definition of center and dispersion, and precision measures are described in the figure legends.

3. Results

3.1. Identification of anti-NRXN1α autoantibodies in patients with schizophrenia

Serum samples were obtained from 362 healthy controls (181 males and 181 females; ages 22–90 years; median, 49 years) and 387 patients with schizophrenia (195 males and 192 females; ages 16–84 years; median, 51 years). Schizophrenia was diagnosed according to the DSM-5 criteria. There were no significant differences in age between the groups.

All samples were tested using a cell-based assay and ELISA. In the cell-based assay using HeLa cells, human NRXN1α and EGFP were expressed from a plasmid, and all transfected cells expressing EGFP showed exogenous expression of NRXN1α (Fig. 1A-B and Supplementary Fig. 1A–B). Eight patients with schizophrenia (2.1%) were positive for anti-NRXN1α autoantibodies (Fig. 1A–B and Supplementary Fig. 1C; Table 1). None of the healthy control participants tested positive for anti-NRXN1α autoantibodies (Fig. 1A). Six of the eight patients whose CSF was examined were positive for anti-NRXN1 antibodies not only in the serum but also in the CSF. (Fig. 1B and Supplementary Fig. 1D; Table 1). The CSF of the other two of the eight patients was not available (Table 1). Protein concentrations and leukocyte numbers in the CSF of these patients were normal. These autoantibodies reacted with NRXN1α expressed by primary cultured neurons (Supplementary Fig. 2A–B) and in the frontal cortex of mice (Supplementary Fig. 2C–D). To test whether these patients also have other autoantibodies against other synaptic molecules, we induced the expression of NCAM1, NLGN1, NLGN2, NLGN3, NLGN4, ephrin B1-B3, ERBB4, NRG1, NR1, NR2, and $GABA_AR\alpha1$ in the same cell-based assay approach. However, no autoantibodies were found against these molecules in these eight schizophrenia patients with anti-NRXN1α autoantibodies (data not shown).

The ELISA analysis detected the same eight patients with schizophrenia (2.1%) as positive for anti-NRXN1α autoantibodies, where two SDs above the mean of absorbance were defined as positive for this autoantibody (Fig. 1C). None of the healthy control participants tested positive for anti-NRXN1α autoantibodies in the ELISA.

The clinical features of the eight patients with anti-NRXN1α autoantibodies detected by cell-based assay are described in Table 1. There were no distinct psychiatric or neurological symptoms in these patients compared with other patients. Furthermore, there was no common past medical history, such as cancer or an autoimmune disease, shared among patients. However, in these patients, psychiatric symptoms including hallucinations and delusions were refractory to antipsychotics. The medications administered to these patients are listed in Supplementary Table 1.

To identify the epitope recognized by the anti-NRXN1α autoantibody, we constructed a truncated form of NRXN1α (Fig. 1D). The extracellular region of NRXN1α comprises six laminins, neurexin, and sex-hormone-binding protein (LNS) domains. The cell-based assay revealed that the serum from the eight patients with schizophrenia reacted with both the truncated forms of ΔLNS1–3 and ΔLNS1–5, which lack the LNS1–3 and LNS1–5 domains, respectively. However, they did not react with those of Δ LNS1–6, which lack the LNS1–6 domains (Fig. 1E–F). These data indicate that the epitope region resides within the LNS6 domain.

We analyzed whether anti-NRXN1α autoantibodies cross-react with other molecules that contain LSN domains, such as NRXN3α and CASPR2. The cell-based assay revealed that none of the anti-NRXN1 α autoantibodies in the eight patients identified by the cell-based assay react with these molecules (Supplementary Fig. 3A–B). These results suggest that anti-NRXN1α autoantibodies react with an NRXN1α-specific sequence.

3.2. Anti-NRXN1α autoantibodies disrupt NRXN1α-NLGN1 and NRXN1α-NLGN2 interactions

NRXN1α is highly expressed in the nervous system. We performed western blot analysis to verify the expression of NRXN1α in mouse brains and found that NRXN1α was indeed expressed at very high levels compared with peripheral organs (Supplementary Fig. 4A). NRXN1α is a presynaptic cell adhesion molecule that forms synapses through

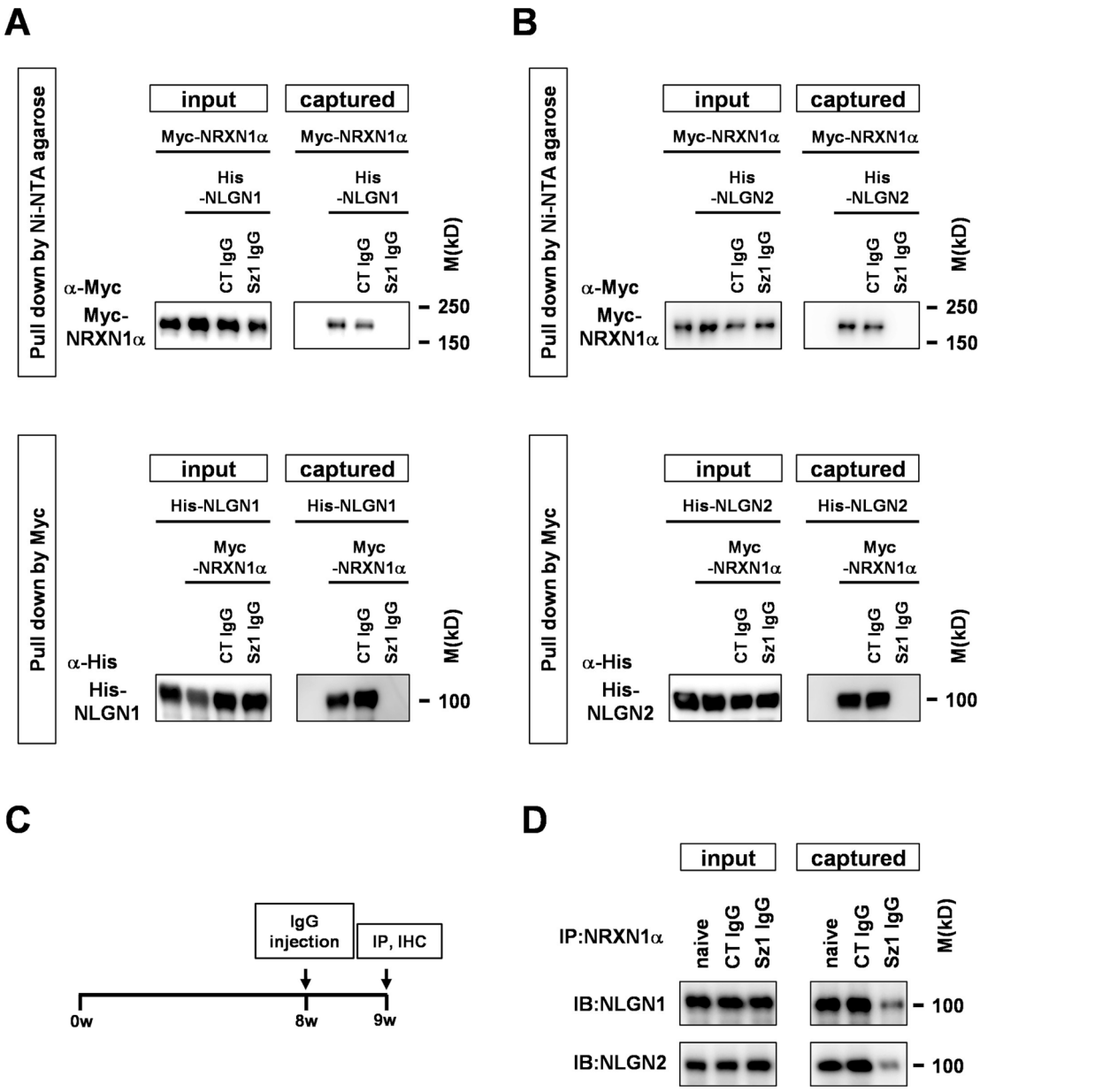

Fig. 2. Anti-NRXN1α autoantibodies disrupt NRXN1α-NLGN1 and NRXN1α-NLGN2 interactions. A. Pull-down assay confirming that IgG purified from the serum of patient 1 with schizophrenia who was positive for anti-NRXN1α autoantibodies disrupt NRXN1α-NLGN1 interactions. His-tagged proteins were pulled down by Ni-NTA-agarose, and Myc-tagged proteins were pulled down by anti-Myc tag beads. B. Pull-down assay confirming that IgG purified from the serum of patient 1 with schizophrenia who was positive for anti-NRXN1α autoantibodies disrupt NRXN1α-NLGN2 interactions. His-tagged proteins were pulled down by Ni-NTA-agarose, and Myc-tagged proteins were pulled down by anti-Myc tag beads. C. Experimental protocol for IgG injection and immunoprecipitation. Purified IgG was injected into the CSF of 8-week-old mice, and immunoprecipitation analysis was performed after 1 week. D. Immunoprecipitation analysis of tissue from the frontal cortex of mice revealed that the NRXN1α-NLGN1 and NRXN1α-NLGN2 interactions were inhibited by anti-NRXN1α autoantibodies present in patients with schizophrenia.

interaction with NLGNs (postsynaptic cell adhesion molecules) via its LNS6 domain (Südhof, 2017). Thus, we hypothesized that anti-NRXN1α autoantibodies would inhibit NRXN1α-NLGN interactions. A pull-down assay showed that IgG purified from the serum of an anti-NRXN1α autoantibody-positive patient with schizophrenia (patient 1) inhibited NRXN1α-NLGN1 and NRXN1α-NLGN2 interactions, whereas IgG purified from the serum of healthy controls did not (Fig. 2A–B). To confirm that anti-NRXN1α antibodies inhibit these interactions *in vivo*, we isolated IgG from anti-NRXN1α autoantibody-positive patients with schizophrenia and from an age- and sex-matched healthy participant. We then injected these antibodies into the CSF of 8-week-old mice and conducted an immunoprecipitation analysis after 1 week (Fig. 2C). Immunohistochemical analysis confirmed that intrathecally administered anti-NRXN1α autoantibodies from patients with schizophrenia were still present in 9-week-old mice (Supplementary Fig. 5B). No evidence on state changes, the polarization of microglia and astrocytes, or encephalitis assessed by the nuclear translocation of NFκB and inflammatory markers such as TNFα and ISG54 was found (Supplementary Fig. 6A–D, Supplementary Fig. 7). Consistent with the findings from the pull-down assay, anti-NRXN1α autoantibodies inhibited NRXN1α-NLGN1 and NRXN1α-NLGN2 interactions (Fig. 2D). A pull-down assay and immunoprecipitation analysis showed that IgG purified from the serum of schizophrenia patients 2 and 3 also inhibited NRXN1α-NLGN1 and NRXN1α-NLGN2 interactions (Supplementary Fig. 4B–E).

3.3. Anti-NRXN1α autoantibodies reduce mEPSC frequency

NRXN1α knockout mice showed a reduced mEPSC frequency (Etherton et al., 2009). If the anti-NRXN1α autoantibodies found in patients with schizophrenia inhibit NRXN1α-NLGN1 and NRXN1α-NLGN2 interactions, we assumed that they would also change the electrophysiological properties of synapses in mice. To test this, we performed an electrophysiological analysis of the mEPSC in the frontal cortex. We found a markedly decreased mEPSC frequency in mice treated with anti-NRXN1α autoantibodies (Fig. 3A–B). However, there were no changes in the mEPSC amplitude (Fig. 3A and C). These data are consistent with previous findings in knockout mice and confirm that

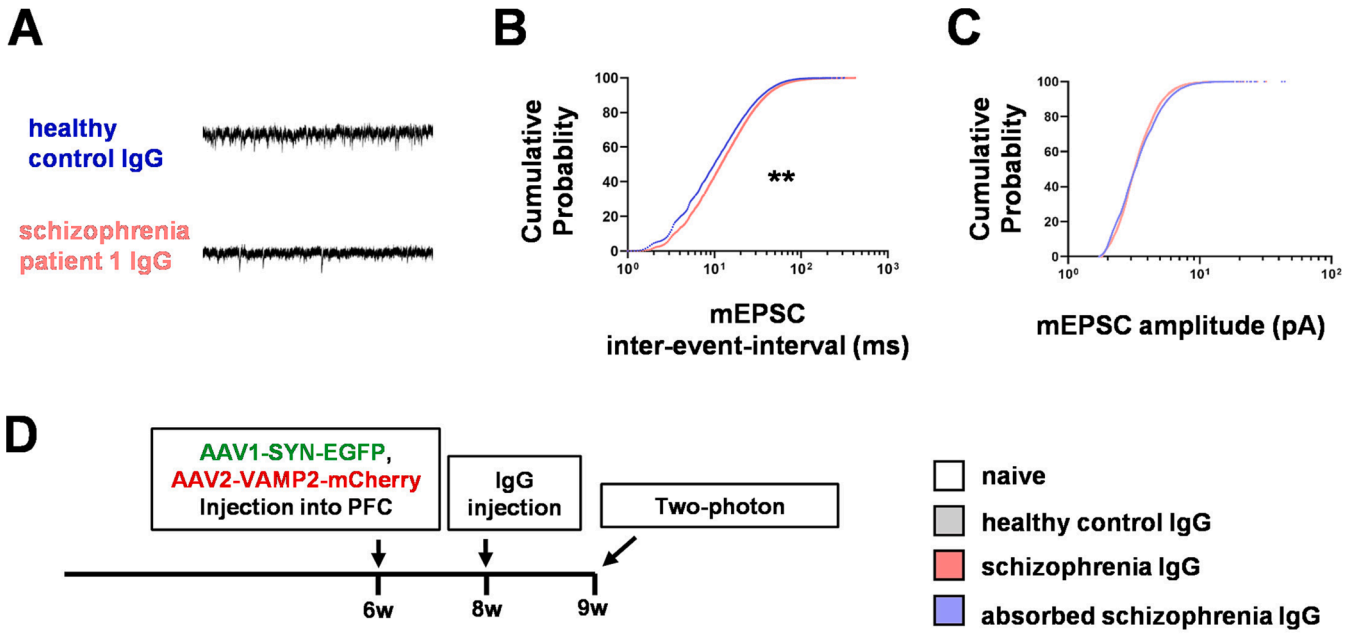

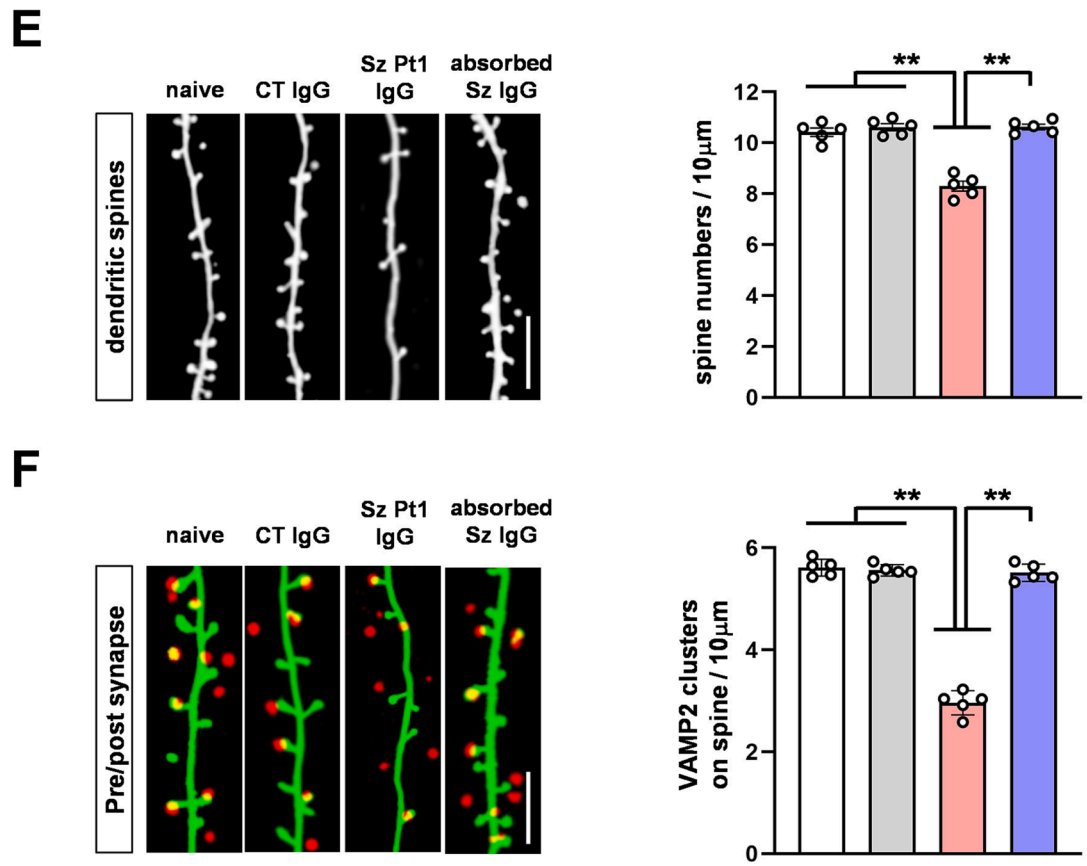

(caption on next page)

Fig. 3. Anti-NRXN1α autoantibodies alter electrophysiological and synaptic properties. A. Representative mEPSC traces were recorded in the frontal cortex pyramidal neurons. B. Cumulative distribution of inter-event intervals for each group. The recording times were 7.5–15 min (a total of 34,523 intervals were detected) and 9.5–10 min (a total of 27,640 intervals were detected) for the healthy control and schizophrenia patient 1, respectively. Nine cells from three mice were analyzed per group. $^{**}p < 0.01$; Kolmogorov–Smirnov test and Mann–Whitney *U* test. C. Cumulative distribution of amplitudes per group. Healthy control, 34,532 amplitudes; patient 1, 27,649 amplitudes. Nine cells from three mice per group were analyzed. $^{**}p < 0.01$; Kolmogorov–Smirnov test and Mann–Whitney *U* test. D. Experimental protocol for IgG injection. AAV1-SYN1-EGFP and AAV2-VAMP2-mCherry were injected into the frontal cortex of 6-week-old mice, and purified IgG was injected into the CSF of 8-week-old mice. Two-photon microscopy analyses were performed on 9-week-old mice. E. Two-photon microscopic images of dendritic spines in the first layer of the frontal cortex of mice injected with AAV1-SYN1-EGFP and IgG purified from the serum of patient 1 with schizophrenia or IgG purified from the serum of healthy control. Removal of anti-NRXN1α antibodies from the purified IgG reversed the decrease in the number of spines. The graph on the right shows a quantitative analysis of the spine number. $^{**}p < 0.01$ ($N = 5$ mice per group; 50 dendrites/mouse; 500 spines/mouse; Tukey's honestly significant difference [HSD] test). Data are expressed as the mean ± s.e.m. Bar: 5 μm. F. Two-photon microscopic images showing contact between axon terminals and dendritic spines in the first layer of the frontal cortex of mice injected with AAV2-VAMP2-mCherry, AAV1-SYN1-EGFP, IgG purified from the serum of patient 1 with schizophrenia, or IgG from a healthy control. The graph on the right shows a quantitative analysis of axon terminals merged with spines. $^{**}p < 0.01$ ($N = 5$ mice per group; 50 dendrites/mouse; 500 spines/mouse; Tukey's HSD test). Data are expressed as the mean ± s.e.m. Bar: 5 μm.

anti-NRXN1α autoantibodies alter electrophysiological synaptic properties (Etherton et al., 2009).

3.4. Anti-NRXN1α autoantibodies reduce the number of synapses and spines

Interactions between NRXN1α and NLGNs are necessary for the formation and maintenance of synapses (Graf et al., 2004; Levinson et al., 2005). These previous findings indicate that anti-NRXN1α autoantibodies may also induce changes in spines and synapses. To examine this, we performed a two-photon analysis on mice that received patient IgG intrathecally. Neurites and spines were visualized using AAV1-EGFP, driven by the synapsin I promoter (AAV1-SYN-EGFP); axon terminals in contact with a spine were visualized using AAV2-VAMP2-mCherry (Fig. 3D). As expected, mice treated with IgG from patient 1 with schizophrenia showed reduced numbers of spines and synapses in the frontal cortex; these changes were not observed in mice that received IgG from a healthy participant (Fig. 3E–F). These changes were replicated in female mice (Supplementary Fig. 8A–C). We also analyzed spine subtypes (filopodia, thin, stubby, and mushroom). There were no significant differences between these subtypes (Supplementary Fig. 9A–B). To confirm the decreased numbers of spines and axon terminals, we conducted immunohistochemistry using markers such as PSD95, gephyrin, vGlut1, and SV2A and found that the number of these puncta is decreased in mice treated with IgG from patient 1 (Supplementary Fig. 9C). The decreased number of gephyrin puncta indicates that anti-NRXN1α autoantibodies affect not only excitatory synapses but also inhibitory synapses.

To confirm that it was the anti-NRXN1α antibodies among IgGs purified from patient 1 that reduced the number of spines and synapses in mice, we performed an absorption experiment in which anti-NRXN1α antibodies were removed from IgG purified from the serum of patient 1 with schizophrenia before administration in mice. Adsorption and removal of anti-NRXN1α antibodies by Myc pull-down were confirmed in a cell-based assay and by immunohistochemistry (Supplementary Fig. 5A–B). The reduction in the number of spines and synapses was reversed after the absorption experiment (Fig. 3E–F). These results confirm that anti-NRXN1α antibodies induce synaptic changes in mice.

3.5. Anti-NRXN1α autoantibodies cause schizophrenia-related behavior in mice

To test whether anti-NRXN1α autoantibodies trigger schizophrenia-related behaviors in mice, we performed a behavioral analysis of autoantibody-treated mice (Fig. 4A). Administration of IgG purified from the serum of patient 1 with schizophrenia reduced cognitive function in the Y-maze test (Fig. 4B). Moreover, these mice were deficient in pre-pulse inhibition, which is an established endophenotype of schizophrenia (Fig. 4C) (Osumi et al., 2015; Powell and Miyakawa, 2006; Powell et al., 2009; Swerdlow et al., 2008). A three-chamber test revealed that autoantibody-treated mice showed a reduced social novelty preference (Fig. 4D). These changes were also replicated in female mice (Supplementary Fig. 8D–F). To confirm that this was not secondary to a memory deficit, we performed a novelty object recognition test. There was no difference between autoantibody-treated mice and control mice in the novelty object recognition test, in which the experimental time frame was similar to that of the three-chamber test (Fig. 4E). This indicates that a reduced social novelty preference was not due to a memory deficit. This interpretation is also consistent with the fact that some disease model mice showed normal social novelty preference behavior in the three-chamber test but showed reduced cognitive function in the Y-maze test (Shiwaku et al., 2022). Mice receiving IgG from patients with schizophrenia showed no abnormal locomotor activity or anxiety behavior in an open-field test, a novelty object recognition test, and an elevated plus maze test (Supplementary Fig. 10A–D). Mice with anti-NRXN1α autoantibodies also did not show obvious aggressive behaviors or olfactory deficits (Supplementary Fig. 10E–F). These data indicate that a reduced social novelty preference was not due to a motor deficit or an olfactory deficit, which is consistent with the previous reports on NRXN1α knockout mice (Armstrong et al., 2020; Grayton et al., 2013). The deficits in the Y-maze test, pre-pulse inhibition, and three-chamber test improved after an absorption experiment in which anti-NRXN1α antibodies were removed from IgG purified from the serum of patient 1 with schizophrenia before administration (Fig. 4B–E).

3.6. Anti-NRXN1α autoantibodies cause schizophrenia-related behavior and alter synapses in mice

Finally, to confirm that the results from schizophrenia patient 1 could be observed in other patients who are positive for anti-NRXN1α autoantibodies, we conducted two-photon and behavioral analyses using IgG purified from the serum of schizophrenia patients 2 and 3 (Fig. 5A). IgG from these patients also decreased the numbers of spines and synapses in the frontal cortex of mice and induced cognitive impairment, pre-pulse inhibition deficiency, and impaired social novelty preference (Fig. 5B–E).

4. Discussion

Here, we identified novel anti-NRXN1α autoantibodies in patients with schizophrenia. Administration of IgG antibodies purified from patients with schizophrenia interrupted NRXN1α-NLGN1 and NRXN1α-NLGN2 interactions. They also reduced the frequency of the mEPSC in the frontal cortex. Furthermore, the administration of anti-NRXN1α antibodies into the CSF of mice reduced the number of spines and synapses in the frontal cortex and caused schizophrenia-related behaviors, inducing cognitive impairment, pre-pulse inhibition deficiency, and impaired social novelty preference.

Dysregulation of synapses and schizophrenia-related behaviors in mice receiving anti-NRXN1α autoantibodies are consistent with findings in NRXN1α knockout mice. NRXN1α knockout mice showed deficient

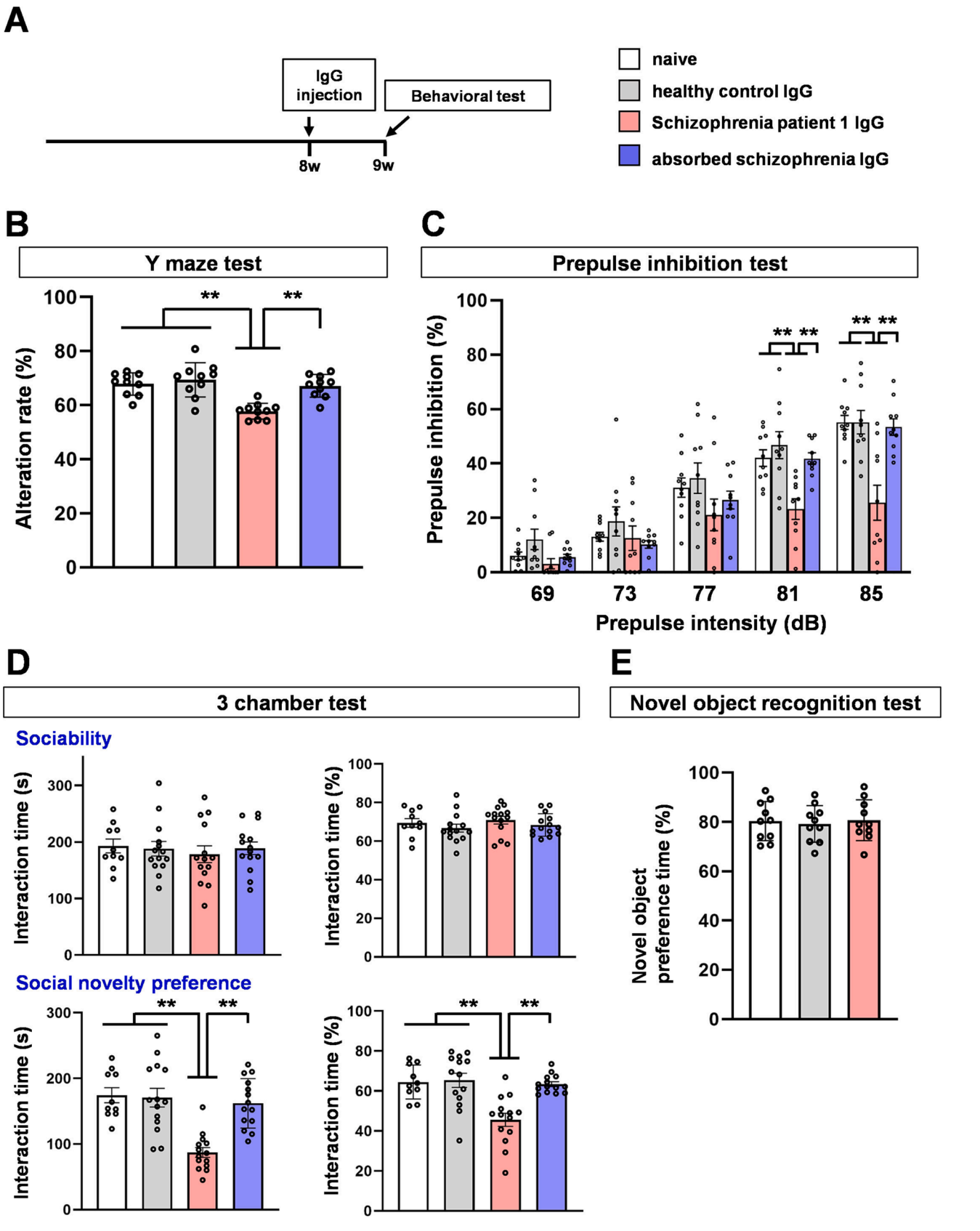

(caption on next page)

Fig. 4. Anti-NRXN1α autoantibodies from a patient with schizophrenia cause schizophrenia-related behavior in mice. A. Experimental protocol for IgG injection. Purified IgG was injected into the CSF of 8-week-old mice, and behavioral analysis was performed after 1 week. B. Alteration ratios in the Y-maze test after injection of purified IgG from patients with schizophrenia or from a healthy control. Removal of anti-NRXN1α antibodies from purified IgG reversed the decrease in the alteration ratios. $^{**}p < 0.01$ ($N = 10$ mice per group, Tukey's HSD test). Data are expressed as the mean ± s.e.m. C. Pre-pulse inhibition rates of mice injected with IgG purified from the serum of patient 1 with schizophrenia or healthy controls. Removal of anti-NRXN1α antibodies from purified IgG reversed the deficiency in pre-pulse inhibition. $^{*}p < 0.05$, $^{**}p < 0.01$ ($N = 10$ mice per group, Tukey's HSD test). Data are expressed as the mean ± s.e.m. D. Sociability and social novelty preference in the three-chamber test. The time (absolute value; left) and percentage (right) taken to approach a cup containing a novel mouse versus the time taken to approach both cups were investigated. Removal of anti-NRXN1α antibodies from purified IgG reversed the reduced social novelty preference. $^{**}p < 0.01$ ($N = 10$–14 mice per group; Tukey's HSD test). E. Novel object recognition test. There was no significant difference between the groups ($N = 10$ mice per group; Tukey's HSD test).

pre-pulse inhibition, altered social interactions, and cognitive impairment (Etherton et al., 2009; Grayton et al., 2013). NRXN1α knockout mice also showed a reduction in mEPSC frequency, which indicates impairment of synaptic transmission as well as a reduced number of synapses (Etherton et al., 2009). This is consistent with our findings of reduced numbers of synapses in anti-NRXN1α autoantibody-treated mice. The difference between NRXN1α knockout mice and anti-NRXN1α autoantibody-treated mice is the absence of obvious aggressive behavior in the latter (Grayton et al., 2013). This discrepancy may stem from the fact that the disruption of molecular binding with NLGN1 and NLGN2 is not complete.

Factors other than NRXN1α dysfunction may cause dysregulation of synapses in the presence of anti-NRXN1α autoantibodies. For example, targeting of synapses by autoantibodies and complement component C1q may result in microglial synaptic pruning. Autoantibodies as targets of C1q have been reported in mouse models of neuropsychiatric systemic lupus erythematosus and neuromyelitis optica (Nestor et al., 2018; Soltys et al., 2019). C1q-mediated synaptic pruning by microglia occurs during normal development (Paolicelli et al., 2011; Stevens et al., 2007). During normal development, synaptic pruning usually terminates during adolescence, whereas the progression of synaptic pruning after adolescence is hypothesized for schizophrenia (Forsyth and Lewis, 2017). Autoantibodies targeting synaptic molecules, including NRXN1α, found in patients with schizophrenia may be involved in such progressive synaptic punning by acting as target markers for C1q and microglia. Similar synaptic pruning is also reported for astrocytes (Chung et al., 2013; Tasdemir-Yilmaz and Freeman, 2014). Although the state changes or the polarization of microglia and astrocytes were not detected in our study in the context of inflammation, synaptic engulfment by microglia or astrocytes without inflammation via autoantibodies will be tested in future studies.

Another thesis for future studies is cross-reactivity. Cross-reactivity to other antigens has been reported for some autoantibodies, such as anti-GABA receptor autoantibodies to LMO5 or anti-NMDA receptor autoantibodies to dsDNA (Brändle et al., 2021; Mader et al., 2017). The use of NRXN1α knockout mice is an approach to elucidate this process. An analysis of cross-reactive antigens could further reveal the pathogenic properties of anti-NRXN1α autoantibodies.

The time period during which anti-NRXN1α autoantibodies are produced in some patients with schizophrenia is also a topic for future research. The transfer of autoantibodies from mother to fetus via the placenta has been implicated in developmental disorders (Coutinho et al., 2021; Coutinho et al., 2017; Marks et al., 2020). The production of anti-NRXN1α autoantibodies during childhood and the disruption of NRXN1α function during the neurodevelopmental period should affect symptoms in adolescence, as shown in a mouse model. The production of autoantibodies during the developmental period or adolescence also relates to whether anti-NRXN1α autoantibodies are involved in the onset of schizophrenia. These issues will be tested in a longitudinal study with a cohort of children and adolescents.

This study has several limitations. First, this study does not show the relationship between anti-NRXN1α autoantibodies and autoimmune encephalitis (AE) or autoimmune psychosis (AP) (Graus et al., 2016; Pollak et al., 2020). More than 20 autoantibodies against the nervous system have been reported, and related psychiatric and cognitive symptoms have also been proposed (Pollak et al., 2020). The disruption of the blood–brain barrier and related genetic background are associated with whether these autoantibodies are linked to the onset of AE and AP (Arinrad et al., 2021; Daguano Gastaldi et al., 2022; Diamond et al., 2009; Hammer et al., 2014). According to the proposed diagnostic criteria for AP (Pollak et al., 2020), our cases with anti-NRXN1α autoantibodies in the CSF may fit the concept of AP; however, the diagnostic criteria also state that "the patient must have current psychotic symptoms of abrupt onset (rapid progression of < 3 months)." Our patient manifested chronic psychosis with schizophrenia, which may not be consistent with this point of the criteria. However, it is possible that the anti-NRXN1α autoantibodies were positive from the onset, and these chronic cases may have been AP at the onset. Furthermore, it should be investigated whether anti-NRXN1α autoantibodies are associated with a more typical AP and AE. Second, the MRI and CSF analyses were brief. Although obvious atrophy or evidence of encephalitis was absent, it is still possible that further CSF and neuroimaging analysis in a larger cohort would better elucidate any pathologies of anti-NRXN1α autoantibodies. Third, although we revealed that anti-NRXN1α autoantibodies can be pathogenic in mice, a study that would elucidate the removal of these autoantibodies from patients is necessary to conclude the extent to which anti-NRXN1α autoantibodies relate to schizophrenia symptoms. Nevertheless, studies showing that autoantibodies cause schizophrenia-related pathologies in mice are a necessary and important step toward clinical studies. Regarding the effect on cognitive function, we found cognitive dysfunction due to the anti-NRXN1α autoantibody in the Y-maze test in mice. The precise effects of anti-NRXN1α autoantibodies on cognitive dysfunction will be revealed by further cognitive behavioral analyses, chronic administration of autoantibodies to mice, and longitudinal cognitive analyses in patients with anti-NRXN1α autoantibodies.

In this study, we discovered that approximately 2.1% of patients have autoantibodies against NRXN1α. Although the prevalence of anti-NRXN1α autoantibodies is low in patients with schizophrenia, the fact that we could not find anti-NRXN1α autoantibodies in controls may increase the importance of these autoantibodies. Furthermore, in our previous study, we demonstrated that approximately 5.4% of patients with schizophrenia are positive for anti-NCAM1 autoantibodies (Shiwaku et al., 2022). No overlap was found between patients with anti-NCAM1 autoantibodies and those with anti-NRXN1α autoantibodies. Thus, at least 7.5% of patients with schizophrenia have autoantibodies against synaptic molecules. This finding indicates that although the percentage of patients who are positive for each autoantibody may be low, the percentage of patients with autoantibodies against any type of synaptic molecule may be substantial. It also indicates the presence of other important autoantibodies in patients with schizophrenia.

In conclusion, we identified anti-NRXN1α autoantibodies in patients with schizophrenia. These antibodies cause changes in synapses and schizophrenia-related behavior in mice. These autoantibodies may cause symptoms of schizophrenia and can therefore be regarded as a therapeutic target/biomarker for a subtype of this disorder.

Author contributions

H.S. designed and supervised the study, performed the experiments, analyzed the data, and wrote the manuscript. H.S., S.K., Y.N., S.T., and

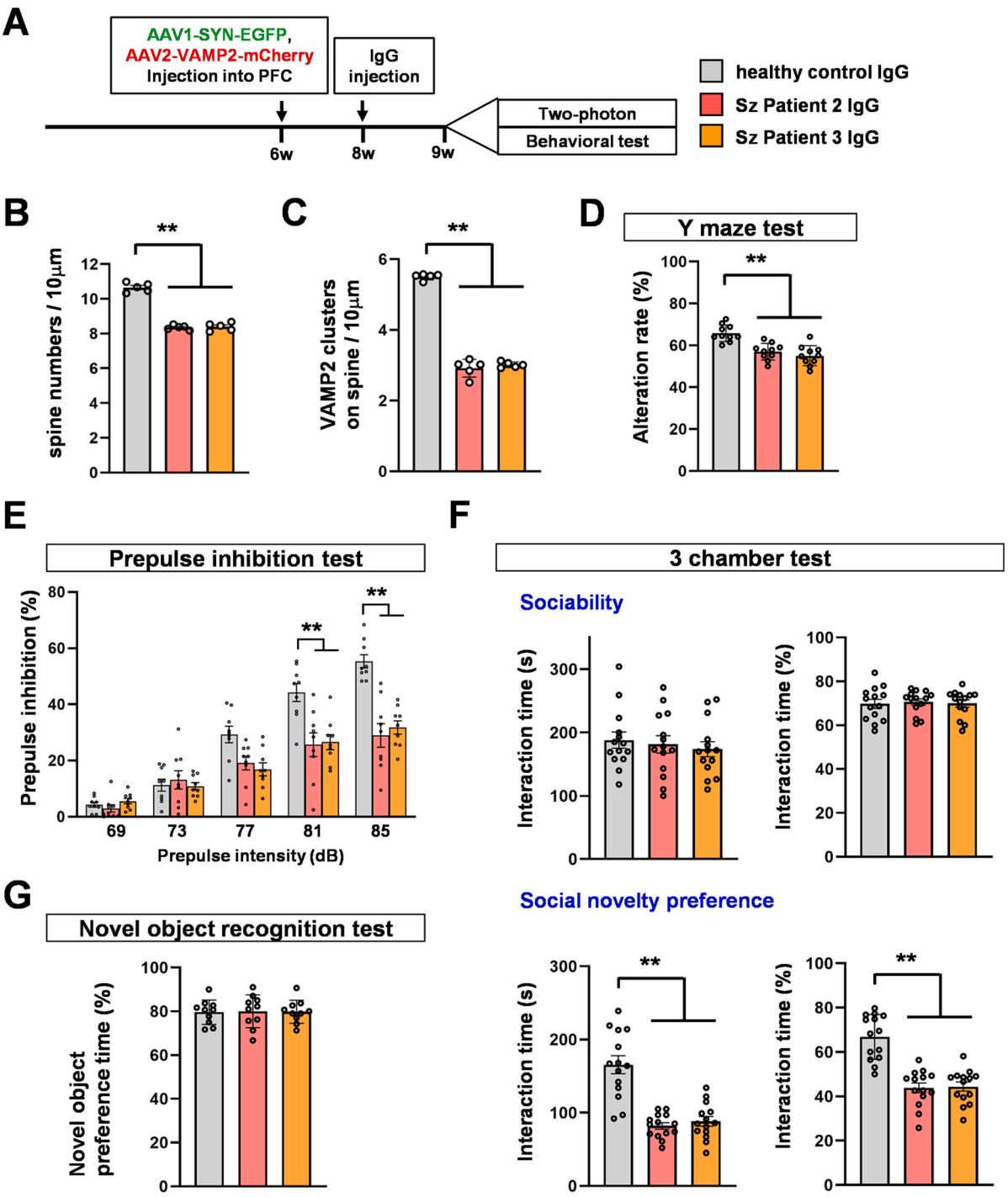

Fig. 5. Autoantibodies from patients with schizophrenia cause schizophrenia-related behavior and changes in synapse numbers in mice. A. Experimental protocol for IgG injection. AAV1-SYN1-EGFP and AAV2-VAMP2-mCherry were injected into the frontal cortex of 6-week-old mice, and purified IgG was injected into the CSF of 8-week-old mice. Two-photon microscopy and behavioral analyses were performed on 9-week-old mice. B. Two-photon microscopic analysis of dendritic spines in the first layer of the frontal cortex of mice injected with AAV1-SYN1-EGFP and IgG purified from the serum of healthy controls, patient 2, and patient 3 with schizophrenia. $^{**}p < 0.01$ ($N = 5$ mice per group; 50 dendrites/mouse; 500 spines/mouse; Tukey's HSD test). Data are expressed as mean ± s.e.m. C. Two-photon microscopic analysis of axon terminals merged with spines in the first layer of the frontal cortex of mice injected with AAV2-VAMP2-mCherry, AAV1-SYN1-EGFP, and IgG purified from the healthy control serum, patient 2, and patient 3 with schizophrenia. $^{**}p < 0.01$ ($N = 5$ mice per group; 50 dendrites/mouse; 500 spines/mouse; Tukey's HSD test). Data are expressed as mean ± s.e.m. Bar: 5 μm. D. Alteration ratios in the Y-maze test after injection of IgG purified from the serum of healthy control, patient 2, and patient 3 with schizophrenia. $^{**}p < 0.01$ ($N = 9$ mice per group, Tukey's HSD test). Data are expressed as mean ± s.e.m. E. Pre-pulse inhibition rates of mice injected with IgG purified from serum of healthy control, patient 2, and patient 3 with schizophrenia. $^{*}p < 0.05$, $^{**}p < 0.01$ ($N = 9$ mice per group, Tukey's HSD test). Data are expressed as mean ± s.e.m. F. Sociability and social novelty preference were assessed in the three-chamber test of mice injected with IgG purified from the serum of healthy control, patient 2, and patient 3 with schizophrenia. $^{**}p < 0.01$ ($N = 10$–14 mice per group; Tukey's HSD test). G. Novel object recognition test. There was no significant difference between the groups ($N = 10$ mice per group; Tukey's HSD test).

Y.M. performed and analyzed the immunocytochemical, immunohistochemical, biochemical, and behavioral experiments. M.G. and Y.I. performed and analyzed the electrophysiological experiments. H.S., S.K., and K.K. performed two-photon experiments. H.S., H.T., F.Y., H.H., H. K., and K.I. collected human samples. T.K., Y.I., H.O., and H.T. supervised the study.

Declaration of Competing Interest

The authors declare that they have no known competing financial interests or personal relationships that could have appeared to influence the work reported in this paper.

Data availability

Data will be made available on request.

Acknowledgments

This work was supported by the Tokyo Biochemical Research Foundation, SENSHIN Medical Research Foundation, a Grant-in-Aid for Scientific Research from Japan Society for Promotion of Science (JSPS) (19K08011, 22K07553), and Japan Agency for Medical Research and Development (AMED) (JP22wm0525036) to H.S., Uehara Memorial Foundation, a Grant-in-Aid for Exploratory Research (20K21567) from JSPS, and a Grant-in-Aid for Scientific Research on Innovative Areas (16H06572) from the Ministry of Education, Culture, Sports, Science and Technology of Japan (MEXT) to H.T., JST ERATO (JPMJER1801), Institute for AI and Beyond of the University of Tokyo and a Grant-in-Aid for Scientific Research No. 18H05525 from JSPS to Y.I. and a Grant-in-Aid for Scientific Research on Innovative Areas (Foundation of Synapse and Neurocircuit Pathology, 22110001/22110002) to H.O. from MEXT.

Appendix A. Supplementary data

Supplementary data to this article can be found online at https://doi.org/10.1016/j.bbi.2023.03.028.

References

Arinrad, S., Wilke, J.B.H., Seelbach, A., Doeren, J., Hindermann, M., Butt, U.J., Steixner-Kumar, A.A., Spieth, L., Ronnenberg, A., Pan, H., Berghoff, S.A., Hollmann, M., Lühder, F., Nave, K.A., Bechter, K., Ehrenreich, H., 2021. NMDAR1 autoantibodies amplify behavioral phenotypes of genetic white matter inflammation: a mild encephalitis model with neuropsychiatric relevance. Mol. Psychiatry.

Armstrong, E.C., Caruso, A., Servadio, M., Andreae, L.C., Trezza, V., Scattoni, M.L., Fernandes, C., 2020. Assessing the developmental trajectory of mouse models of neurodevelopmental disorders: Social and communication deficits in mice with Neurexin 1α deletion. Genes Brain Behav. 19, e12630.

Brändle, S.M., Cerina, M., Weber, S., Held, K., Menke, A.F., Alcalá, C., Gebert, D., Herrmann, A.M., Pellkofer, H., Gerdes, L.A., Bittner, S., Leypoldt, F., Teegen, B., Komorowski, L., Kümpfel, T., Hohlfeld, R., Meuth, S.G., Casanova, B., Melzer, N., Beltrán, E., Dornmair, K., 2021. Cross-reactivity of a pathogenic autoantibody to a tumor antigen in GABA(A) receptor encephalitis. Proc Natl Acad Sci U S A 118.

Chung, W.S., Clarke, L.E., Wang, G.X., Stafford, B.K., Sher, A., Chakraborty, C., Joung, J., Foo, L.C., Thompson, A., Chen, C., Smith, S.J., Barres, B.A., 2013. Astrocytes mediate synapse elimination through MEGF10 and MERTK pathways. Nature 504, 394–400.

Coutinho, E., Menassa, D.A., Jacobson, L., West, S.J., Domingos, J., Moloney, T.C., Lang, B., Harrison, P.J., Bennett, D.L.H., Bannerman, D., Vincent, A., 2017. Persistent microglial activation and synaptic loss with behavioral abnormalities in mouse offspring exposed to CASPR2-antibodies in utero. Acta Neuropathol. 134, 567–583.

Coutinho, E., Jacobson, L., Shock, A., Smith, B., Vernon, A., Vincent, A., 2021. Inhibition of maternal-to-fetal transfer of IgG antibodies by FcRn blockade in a mouse model of arthrogryposis multiplex congenita. Neurol Neuroimmunol. Neuroinflamm. 8.

Cullen, A.E., Holmes, S., Pollak, T.A., Blackman, G., Joyce, D.W., Kempton, M.J., Murray, R.M., McGuire, P., Mondelli, V., 2019. Associations Between non-neurological autoimmune disorders and psychosis: A meta-analysis. Biol. Psychiatry 85, 35–48.

Daguano Gastaldi, V., Bh Wilke, J., Weidinger, C.A., Walter, C., Barnkothe, N., Teegen, B., Luessi, F., Stöcker, W., Lühder, F., Begemann, M., Zipp, F., Nave, K.A., Ehrenreich, H., 2022. Factors predisposing to humoral autoimmunity against brain-antigens in health and disease Analysis of 49 autoantibodies in over 7000 subjects. Brain Behav. Immun.

Dalmau, J., 2016. NMDA receptor encephalitis and other antibody-mediated disorders of the synapse: The 2016 Cotzias Lecture. Neurology 87, 2471–2482.

Dean, C., Dresbach, T., 2006. Neuroligins and neurexins: linking cell adhesion, synapse formation and cognitive function. Trends Neurosci. 29, 21–29.

Diamond, B., Huerta, P.T., Mina-Osorio, P., Kowal, C., Volpe, B.T., 2009. Losing your nerves? Maybe it's the antibodies. Nat. Rev. Immunol. 9, 449–456.

Etherton, M.R., Blaiss, C.A., Powell, C.M., Südhof, T.C., 2009. Mouse neurexin-1alpha deletion causes correlated electrophysiological and behavioral changes consistent with cognitive impairments. PNAS 106, 17998–18003.

Forsyth, J.K., Lewis, D.A., 2017. Mapping the Consequences of Impaired Synaptic Plasticity in Schizophrenia through Development: An Integrative Model for Diverse Clinical Features. Trends Cogn. Sci. 21, 760–778.

Graf, E.R., Zhang, X., Jin, S.X., Linhoff, M.W., Craig, A.M., 2004. Neurexins induce differentiation of GABA and glutamate postsynaptic specializations via neuroligins. Cell 119, 1013–1026.

Graus, F., Titulaer, M.J., Balu, R., Benseler, S., Bien, C.G., Cellucci, T., Cortese, I., Dale, R. C., Gelfand, J.M., Geschwind, M., Glaser, C.A., Honnorat, J., Höftberger, R., Iizuka, T., Irani, S.R., Lancaster, E., Leypoldt, F., Prüss, H., Rae-Grant, A., Reindl, M., Rosenfeld, M.R., Rostásy, K., Saiz, A., Venkatesan, A., Vincent, A., Wandinger, K.P., Waters, P., Dalmau, J., 2016. A clinical approach to diagnosis of autoimmune encephalitis. Lancet Neurol. 15, 391–404.

Grayton, H.M., Missler, M., Collier, D.A., Fernandes, C., 2013. Altered social behaviours in neurexin 1α knockout mice resemble core symptoms in neurodevelopmental disorders. PLoS One 8, e67114.

Hammer, C., Stepniak, B., Schneider, A., Papiol, S., Tantra, M., Begemann, M., Sirén, A. L., Pardo, L.A., Sperling, S., Mohd Jofrry, S., Gurvich, A., Jensen, N., Ostmeier, K., Lühder, F., Probst, C., Martens, H., Gillis, M., Saher, G., Assogna, F., Spalletta, G., Stöcker, W., Schulz, T.F., Nave, K.A., Ehrenreich, H., 2014. Neuropsychiatric disease relevance of circulating anti-NMDA receptor autoantibodies depends on blood-brain barrier integrity. Mol. Psychiatry 19, 1143–1149.

Hu, Z., Xiao, X., Zhang, Z., Li, M., 2019. Genetic insights and neurobiological implications from NRXN1 in neuropsychiatric disorders. Mol. Psychiatry 24, 1400–1414.

Levinson, J.N., Chéry, N., Huang, K., Wong, T.P., Gerrow, K., Kang, R., Prange, O., Wang, Y.T., El-Husseini, A., 2005. Neuroligins mediate excitatory and inhibitory synapse formation: involvement of PSD-95 and neurexin-1beta in neuroligin-induced synaptic specificity. J. Biol. Chem. 280, 17312–17319.

Lowther, C., Speevak, M., Armour, C.M., Goh, E.S., Graham, G.E., Li, C., Zeesman, S., Nowaczyk, M.J., Schultz, L.A., Morra, A., Nicolson, R., Bikangaga, P., Samdup, D., Zaazou, M., Boyd, K., Jung, J.H., Siu, V., Rajguru, M., Goobie, S., Tarnopolsky, M.A., Prasad, C., Dick, P.T., Hussain, A.S., Walinga, M., Reijenga, R.G., Gazzellone, M., Lionel, A.C., Marshall, C.R., Scherer, S.W., Stavropoulos, D.J., McCready, E., Bassett, A.S., 2017. Molecular characterization of NRXN1 deletions from 19,263 clinical microarray cases identifies exons important for neurodevelopmental disease expression. Genet. Med. 19, 53–61.

Mader, S., Brimberg, L., Diamond, B., 2017. The Role of Brain-Reactive Autoantibodies in Brain Pathology and Cognitive Impairment. Front. Immunol. 8, 1101.

Marks, K., Vincent, A., Coutinho, E., 2020. Maternal-Autoantibody-Related (MAR) Autism: Identifying Neuronal Antigens and Approaching Prospects for Intervention. J. Clin. Med. 9.

Marshall, C.R., Howrigan, D.P., Merico, D., Thiruvahindrapuram, B., Wu, W., Greer, D.S., Antaki, D., Shetty, A., Holmans, P.A., Pinto, D., Gujral, M., Brandler, W.M., Malhotra, D., Wang, Z., Fajarado, K.V.F., Maile, M.S., Ripke, S., Agartz, I., Albus, M., Alexander, M., Amin, F., Atkins, J., Bacanu, S.A., Belliveau Jr., R.A., Bergen, S.E., Bertalan, M., Bevilacqua, E., Bigdeli, T.B., Black, D.W., Bruggeman, R., Buccola, N. G., Buckner, R.L., Bulik-Sullivan, B., Byerley, W., Cahn, W., Cai, G., Cairns, M.J., Campion, D., Cantor, R.M., Carr, V.J., Carrera, N., Catts, S.V., Chambert, K.D., Cheng, W., Cloninger, C.R., Cohen, D., Cormican, P., Craddock, N., Crespo-Facorro, B., Crowley, J.J., Curtis, D., Davidson, M., Davis, K.L., Degenhardt, F., Del Favero, J., DeLisi, L.E., Dikeos, D., Dinan, T., Djurovic, S., Donohoe, G., Drapeau, E., Duan, J., Dudbridge, F., Eichhammer, P., Eriksson, J., Escott-Price, V., Essioux, L., Fanous, A.H., Farh, K.H., Farrell, M.S., Frank, J., Franke, L., Freedman, R., Freimer, N.B., Friedman, J.I., Forstner, A.J., Fromer, M., Genovese, G., Georgieva, L., Gershon, E.S., Giegling, I., Giusti-Rodríguez, P., Godard, S., Goldstein, J.I., Gratten, J., de Haan, L., Hamshere, M.L., Hansen, M., Hansen, T., Haroutunian, V., Hartmann, A.M., Henskens, F.A., Herms, S., Hirschhorn, J.N., Hoffmann, P., Hofman, A., Huang, H., Ikeda, M., Joa, I., Kähler, A.K., Kahn, R.S., Kalaydjieva, L., Karjalainen, J., Kavanagh, D., Keller, M.C., Kelly, B.J., Kennedy, J.L., Kim, Y., Knowles, J.A., Konte, B., Laurent, C., Lee, P., Lee, S.H., Legge, S.E., Lerer, B., Levy, D. L., Liang, K.Y., Lieberman, J., Lönnqvist, J., Loughland, C.M., Magnusson, P.K.E., Maher, B.S., Maier, W., Mallet, J., Mattheisen, M., Mattingsdal, M., McCarley, R.W., McDonald, C., McIntosh, A.M., Meier, S., Meijer, C.J., Melle, I., Mesholam-Gately, R. I., Metspalu, A., Michie, P.T., Milani, L., Milanova, V., Mokrab, Y., Morris, D.W., Müller-Myhsok, B., Murphy, K.C., Murray, R.M., Myin-Germeys, I., Nenadic, I., Nertney, D.A., Nestadt, G., Nicodemus, K.K., Nisenbaum, L., Nordin, A., O'Callaghan, E., O'Dushlaine, C., Oh, S.Y., Olincy, A., Olsen, L., O'Neill, F.A., Van Os, J., Pantelis, C., Papadimitriou, G.N., Parkhomenko, E., Pato, M.T., Paunio, T., Perkins, D.O., Pers, T.H., Pietiläinen, O., Pimm, J., Pocklington, A.J., Powell, J., Price, A., Pulver, A.E., Purcell, S.M., Quested, D., Rasmussen, H.B., Reichenberg, A., Reimers, M.A., Richards, A.L., Roffman, J.L., Roussos, P., Ruderfer, D.M., Salomaa, V., Sanders, A.R., Savitz, A., Schall, U., Schulze, T.G., Schwab, S.G., Scolnick, E.M., Scott, R.J., Seidman, L.J., Shi, J., Silverman, J.M., Smoller, J.W., Söderman, E., Spencer, C.C.A., Stahl, E.A., Strengman, E., Strohmaier, J., Stroup, T. S., Suvisaari, J., Svrakic, D.M., Szatkiewicz, J.P., Thirumalai, S., Tooney, P.A., Veijola, J., Visscher, P.M., Waddington, J., Walsh, D., Webb, B.T., Weiser, M., Wildenauer, D.B., Williams, N.M., Williams, S., Witt, S.H., Wolen, A.R., Wormley, B.

K., Wray, N.R., Wu, J.Q., Zai, C.C., Adolfsson, R., Andreassen, O.A., Blackwood, D.H. R., Bramon, E., Buxbaum, J.D., Cichon, S., Collier, D.A., Corvin, A., Daly, M.J., Darvasi, A., Domenici, E., Esko, T., Gejman, P.V., Gill, M., Gurling, H., Hultman, C. M., Iwata, N., Jablensky, A.V., Jönsson, E.G., Kendler, K.S., Kirov, G., Knight, J., Levinson, D.F., Li, Q.S., McCarroll, S.A., McQuillin, A., Moran, J.L., Mowry, B.J., Nöthen, M.M., Ophoff, R.A., Owen, M.J., Palotie, A., Pato, C.N., Petryshen, T.L., Posthuma, D., Rietschel, M., Riley, B.P., Rujescu, D., Sklar, P., St Clair, D., Walters, J. T.R., Werge, T., Sullivan, P.F., O'Donovan, M.C., Scherer, S.W., Neale, B.M., Sebat, J., 2017. Contribution of copy number variants to schizophrenia from a genome-wide study of 41,321 subjects. Nat. Genet. 49, 27–35.

Meyer-Lindenberg, A., 2010. From maps to mechanisms through neuroimaging of schizophrenia. Nature 468, 194–202.

Nestor, J., Arinuma, Y., Huerta, T.S., Kowal, C., Nasiri, E., Kello, N., Fujieda, Y., Bialas, A., Hammond, T., Sriram, U., Stevens, B., Huerta, P.T., Volpe, B.T., Diamond, B., 2018. Lupus antibodies induce behavioral changes mediated by microglia and blocked by ACE inhibitors. J. Exp. Med. 215, 2554–2566.

Osumi, N., Guo, N., Matsumata, M., Yoshizaki, K., 2015. Neurogenesis and sensorimotor gating: bridging a microphenotype and an endophenotype. Curr. Mol. Med. 15, 129–137.

Paolicelli, R.C., Bolasco, G., Pagani, F., Maggi, L., Scianni, M., Panzanelli, P., Giustetto, M., Ferreira, T.A., Guiducci, E., Dumas, L., Ragozzino, D., Gross, C.T., 2011. Synaptic pruning by microglia is necessary for normal brain development. Science 333, 1456–1458.

Pardridge, W.M., 2016. CSF, blood-brain barrier, and brain drug delivery. Expert Opin. Drug Deliv. 13, 963–975.

Pettingill, P., Kramer, H.B., Coebergh, J.A., Pettingill, R., Maxwell, S., Nibber, A., Malaspina, A., Jacob, A., Irani, S.R., Buckley, C., Beeson, D., Lang, B., Waters, P., Vincent, A., 2015. Antibodies to GABAA receptor α1 and γ2 subunits: clinical and serologic characterization. Neurology 84, 1233–1241.

Pollak, T.A., Lennox, B.R., Müller, S., Benros, M.E., Prüss, H., Tebartz van Elst, L., Klein, H., Steiner, J., Frodl, T., Bogerts, B., Tian, L., Groc, L., Hasan, A., Baune, B.T., Endres, D., Haroon, E., Yolken, R., Benedetti, F., Halaris, A., Meyer, J.H., Stassen, H., Leboyer, M., Fuchs, D., Otto, M., Brown, D.A., Vincent, A., Najjar, S., Bechter, K., 2020. Autoimmune psychosis: an international consensus on an approach to the diagnosis and management of psychosis of suspected autoimmune origin. Lancet Psychiatry 7, 93–108.

Powell, C.M., Miyakawa, T., 2006. Schizophrenia-relevant behavioral testing in rodent models: a uniquely human disorder? Biol. Psychiatry 59, 1198–1207.

Powell, S.B., Zhou, X., Geyer, M.A., 2009. Prepulse inhibition and genetic mouse models of schizophrenia. Behav. Brain Res. 204, 282–294.

Prüss, H., 2021. Autoantibodies in neurological disease. Nat. Rev. Immunol. 1–16.

S.W.G.o.t.P.G. Consortium, 2014. Biological insights from 108 schizophrenia-associated genetic loci. Nature 511, 421–427.

Shiwaku, H., Nakano, Y., Kato, M., Takahashi, H., 2020. Detection of autoantibodies against GABA(A)Rα1 in patients with schizophrenia. Schizophr. Res. 216, 543–546.

Shiwaku, H., Katayama, S., Kondo, K., Nakano, Y., Tanaka, H., Yoshioka, Y., Fujita, K., Tamaki, H., Takebayashi, H., Terasaki, O., Nagase, Y., Nagase, T., Kubota, T., Ishikawa, K., Okazawa, H., Takahashi, H., 2022. Autoantibodies against NCAM1 from patients with schizophrenia cause schizophrenia-related behavior and changes in synapses in mice. Cell Rep Med 3, 100597.

Singh, T., Poterba, T., Curtis, D., Akil, H., Al Eissa, M., Barchas, J.D., Bass, N., Bigdeli, T. B., Breen, G., Bromet, E.J., Buckley, P.F., Bunney, W.E., Bybjerg-Grauholm, J., Byerley, W.F., Chapman, S.B., Chen, W.J., Churchhouse, C., Craddock, N., Cusick, C. M., DeLisi, L., Dodge, S., Escamilla, M.A., Eskelinen, S., Fanous, A.H., Faraone, S.V., Fiorentino, A., Francioli, L., Gabriel, S.B., Gage, D., Gagliano Taliun, S.A., Ganna, A., Genovese, G., Glahn, D.C., Grove, J., Hall, M.H., Hämäläinen, E., Heyne, H.O., Holi, M., Hougaard, D.M., Howrigan, D.P., Huang, H., Hwu, H.G., Kahn, R.S., Kang, H.M., Karczewski, K.J., Kirov, G., Knowles, J.A., Lee, F.S., Lehrer, D.S., Lescai, F., Malaspina, D., Marder, S.R., McCarroll, S.A., McIntosh, A.M., Medeiros, H., Milani, L., Morley, C.P., Morris, D.W., Mortensen, P.B., Myers, R.M., Nordentoft, M., O'Brien, N.L., Olivares, A.M., Ongur, D., Ouwehand, W.H., Palmer, D.S., Paunio, T., Quested, D., Rapaport, M.H., Rees, E., Rollins, B., Satterstrom, F.K., Schatzberg, A., Scolnick, E., Scott, L.J., Sharp, S.I., Sklar, P., Smoller, J.W., Sobell, J.L., Solomonson, M., Stahl, E.A., Stevens, C.R., Suvisaari, J., Tiao, G., Watson, S.J., Watts, N.A., Blackwood, D.H., Børglum, A.D., Cohen, B.M., Corvin, A.P., Esko, T., Freimer, N.B., Glatt, S.J., Hultman, C.M., McQuillin, A., Palotie, A., Pato, C.N., Pato, M.T., Pulver, A.E., St Clair, D., Tsuang, M.T., Vawter, M. P., Walters, J.T., Werge, T.M., Ophoff, R.A., Sullivan, P.F., Owen, M.J., Boehnke, M., O'Donovan, M.C., Neale, B.M., Daly, M.J., 2022. Rare coding variants in ten genes confer substantial risk for schizophrenia. Nature 604, 509–516.

Soltys, J., Liu, Y., Ritchie, A., Wemlinger, S., Schaller, K., Schumann, H., Owens, G.P., Bennett, J.L., 2019. Membrane assembly of aquaporin-4 autoantibodies regulates classical complement activation in neuromyelitis optica. J. Clin. Invest. 129, 2000–2013.

Steiner, J., Walter, M., Glanz, W., Sarnyai, Z., Bernstein, H.G., Vielhaber, S., Kästner, A., Skalej, M., Jordan, W., Schiltz, K., Klingbeil, C., Wandinger, K.P., Bogerts, B., Stoecker, W., 2013. Increased prevalence of diverse N-methyl-D-aspartate glutamate receptor antibodies in patients with an initial diagnosis of schizophrenia: specific relevance of IgG NR1a antibodies for distinction from N-methyl-D-aspartate glutamate receptor encephalitis. JAMA Psychiat. 70, 271–278.

Stevens, B., Allen, N.J., Vazquez, L.E., Howell, G.R., Christopherson, K.S., Nouri, N., Micheva, K.D., Mehalow, A.K., Huberman, A.D., Stafford, B., Sher, A., Litke, A.M., Lambris, J.D., Smith, S.J., John, S.W., Barres, B.A., 2007. The classical complement cascade mediates CNS synapse elimination. Cell 131, 1164–1178.

Südhof, T.C., 2017. Synaptic neurexin complexes: A Molecular code for the logic of neural circuits. Cell 171, 745–769.

Swerdlow, N.R., Weber, M., Qu, Y., Light, G.A., Braff, D.L., 2008. Realistic expectations of prepulse inhibition in translational models for schizophrenia research. Psychopharmacology (Berl) 199, 331–388.

Szatmari, P., Paterson, A.D., Zwaigenbaum, L., Roberts, W., Brian, J., Liu, X.Q., Vincent, J.B., Skaug, J.L., Thompson, A.P., Senman, L., Feuk, L., Qian, C., Bryson, S. E., Jones, M.B., Marshall, C.R., Scherer, S.W., Vieland, V.J., Bartlett, C., Mangin, L. V., Goedken, R., Segre, A., Pericak-Vance, M.A., Cuccaro, M.L., Gilbert, J.R., Wright, H.H., Abramson, R.K., Betancur, C., Bourgeron, T., Gillberg, C., Leboyer, M., Buxbaum, J.D., Davis, K.L., Hollander, E., Silverman, J.M., Hallmayer, J., Lotspeich, L., Sutcliffe, J.S., Haines, J.L., Folstein, S.E., Piven, J., Wassink, T.H., Sheffield, V., Geschwind, D.H., Bucan, M., Brown, W.T., Cantor, R.M., Constantino, J.N., Gilliam, T.C., Herbert, M., Lajonchere, C., Ledbetter, D.H., Lese-Martin, C., Miller, J., Nelson, S., Samango-Sprouse, C.A., Spence, S., State, M., Tanzi, R.E., Coon, H., Dawson, G., Devlin, B., Estes, A., Flodman, P., Klei, L., McMahon, W.M., Minshew, N., Munson, J., Korvatska, E., Rodier, P.M., Schellenberg, G.D., Smith, M., Spence, M.A., Stodgell, C., Tepper, P.G., Wijsman, E. M., Yu, C.E., Rogé, B., Mantoulan, C., Wittemeyer, K., Poustka, A., Felder, B., Klauck, S.M., Schuster, C., Poustka, F., Bölte, S., Feineis-Matthews, S., Herbrecht, E., Schmötzer, G., Tsiantis, J., Papanikolaou, K., Maestrini, E., Bacchelli, E., Blasi, F., Carone, S., Toma, C., Van Engeland, H., de Jonge, M., Kemner, C., Koop, F., Langemeijer, M., Hijmans, C., Staal, W.G., Baird, G., Bolton, P.F., Rutter, M.L., Weisblatt, E., Green, J., Aldred, C., Wilkinson, J.A., Pickles, A., Le Couteur, A., Berney, T., McConachie, H., Bailey, A.J., Francis, K., Honeyman, G., Hutchinson, A., Parr, J.R., Wallace, S., Monaco, A.P., Barnby, G., Kobayashi, K., Lamb, J.A., Sousa, I., Sykes, N., Cook, E.H., Guter, S.J., Leventhal, B.L., Salt, J., Lord, C., Corsello, C., Hus, V., Weeks, D.E., Volkmar, F., Tauber, M., Fombonne, E., Shih, A., Meyer, K.J., 2007. Mapping autism risk loci using genetic linkage and chromosomal rearrangements. Nat. Genet. 39, 319–328.

Tanaka, H., Kondo, K., Chen, X., Homma, H., Tagawa, K., Kerever, A., Aoki, S., Saito, T., Saido, T., Muramatsu, S.I., Fujita, K., Okazawa, H., 2018. The intellectual disability gene PQBP1 rescues Alzheimer's disease pathology. Mol. Psychiatry 23, 2090–2110.

Tasdemir-Yilmaz, O.E., Freeman, M.R., 2014. Astrocytes engage unique molecular programs to engulf pruned neuronal debris from distinct subsets of neurons. Genes Dev. 28, 20–33.

Tromp, A., Mowry, B., Giacomotto, J., 2021. Neurexins in autism and schizophrenia-a review of patient mutations, mouse models and potential future directions. Mol. Psychiatry 26, 747–760.

Vrijenhoek, T., Buizer-Voskamp, J.E., van der Stelt, I., Strengman, E., Sabatti, C., Geurts van Kessel, A., Brunner, H.G., Ophoff, R.A., Veltman, J.A., 2008. Recurrent CNVs disrupt three candidate genes in schizophrenia patients. Am. J. Hum. Genet. 83, 504–510.

Walsh, T., McClellan, J.M., McCarthy, S.E., Addington, A.M., Pierce, S.B., Cooper, G.M., Nord, A.S., Kusenda, M., Malhotra, D., Bhandari, A., Stray, S.M., Rippey, C.F., Roccanova, P., Makarov, V., Lakshmi, B., Findling, R.L., Sikich, L., Stromberg, T., Merriman, B., Gogtay, N., Butler, P., Eckstrand, K., Noory, L., Gochman, P., Long, R., Chen, Z., Davis, S., Baker, C., Eichler, E.E., Meltzer, P.S., Nelson, S.F., Singleton, A. B., Lee, M.K., Rapoport, J.L., King, M.C., Sebat, J., 2008. Rare structural variants disrupt multiple genes in neurodevelopmental pathways in schizophrenia. Science 320, 539–543.

Yang, G., Pan, F., Parkhurst, C.N., Grutzendler, J., Gan, W.B., 2010. Thinned-skull cranial window technique for long-term imaging of the cortex in live mice. Nat. Protoc. 5, 201–208.

Zahir, F.R., Baross, A., Delaney, A.D., Eydoux, P., Fernandes, N.D., Pugh, T., Marra, M.A., Friedman, J.M., 2008. A patient with vertebral, cognitive and behavioural abnormalities and a de novo deletion of NRXN1alpha. J. Med. Genet. 45, 239–243.